

Quantum computing via defect states in two-dimensional anti-dot lattices

Christian Flindt,* Niels Asger Mortensen, and Antti-Pekka Jauho

*MIC – Department of Micro and Nanotechnology,
NanoDTU, Technical University of Denmark,
Building 345east, DK-2800 Kongens Lyngby, Denmark*

(Dated: December 14, 2005)

We propose a new structure suitable for quantum computing in a solid state environment: designed defect states in antidot lattices superimposed on a two-dimensional electron gas at a semiconductor heterostructure. State manipulation can be obtained with gate control. Model calculations indicate that it is feasible to fabricate structures whose energy level structure is robust against thermal dephasing.

At present an intensive search is taking place for solid-state structures which are suitable for quantum computing; a typical example consists of gate-defined double-dot systems studied by several groups [1, 2, 3, 4, 5, 6]. A necessary requirement for a practical application is scalability [7], and many of the existing structures do not immediately offer this possibility. Here we propose an alternative scheme: quantum-mechanical bound states which form at defects in an anti-dot superlattice defined on a semiconductor heterostructure. Scalability is not a critical issue for the suggested structures, which enable the fabrication of a large number of solid-state qubits with no particular extra effort. The flexibility offered by e-beam or local oxidation techniques allows the sample designer to optimize the samples for many different purposes with a very high degree of control.

Anti-dot lattices on semiconductor heterostructures have been a topic of intense research due to their interesting transport properties. In the semiclassical regime novel oscillatory features in magnetoresistance have been discovered [8], and as the lattice spacing is diminished and the quantum regime is approached, exotic energy spectra, such as the Hofstadter butterfly [9] may become experimentally accessible. The fabrication of anti-dot lattices with lattice constants as small as 75 nm has been demonstrated in experiments [10]. Smaller lattice constants are however expected to be within experimental reach [11] leading to a further enhancement of quantum effects. We shall in this paper demonstrate that state-of-the-art anti-dot lattices may have important practical applications in quantum information processing.

Consider a two-dimensional electron gas (2DEG) at a GaAs heterostructure [12] superimposed with a triangular lattice of anti-dots with lattice constant Λ . In the effective-mass approximation the two-dimensional single-electron Schrödinger equation reads

$$\left[-\frac{\hbar^2}{2m^*} \nabla_{\mathbf{r}}^2 + \sum_i V(\mathbf{r} - \mathbf{R}_i) \right] \psi_n(\mathbf{r}) = E_n \psi_n(\mathbf{r}), \quad (1)$$

where the sum runs over all anti-dots i , positioned at \mathbf{R}_i .

Each anti-dot is modelled as a circular potential barrier of height V_0 and diameter d , *i.e.* $V(\mathbf{r}) = V_0$ for $r < d/2$, and zero elsewhere. It is convenient to express all energies in terms of the length scale Λ . Assuming that V_0 is so large that the eigenfunctions ψ_n do not penetrate into the anti-dots, *i.e.* $\psi_n = 0$ in the anti-dots, Eq. (1) simplifies to [13]

$$-\Lambda^2 \nabla_{\mathbf{r}}^2 \psi_n(\mathbf{r}) = \varepsilon_n \psi_n(\mathbf{r}), \quad (2)$$

where we have introduced the dimensionless eigenenergies $\varepsilon_n \equiv E_n \Lambda^2 2m^* / \hbar^2$. For GaAs $\hbar^2 / 2m^* \simeq 0.6$ eVnm².

We first consider the perfectly periodic structure defined by the Wigner-Seitz cell shown in the left inset of Fig. 1. For definiteness, we now take $d/\Lambda = 0.5$. Imposing periodic boundary conditions leaves us with the problem of solving Eq. (2) on a finite-size domain. This class of problems is well-suited for finite-element calculations, and the available software packages make the required computations simple, convenient, and fast [14]. Fig. 1 shows finite-element calculations of the bandstructure along the high-symmetry axes indicated in the right inset of the figure. For state-of-the-art samples $\Lambda \simeq 75$ nm, implying a band-splitting of the order of 3 meV between the two lowest bands at the Γ -point. On the figure we have also indicated the gap ϑ_{eff} below which no states exist for the periodic structure.

Next, we turn to the case where a single anti-dot has been left out of the lattice. Relying on the analogy with photonic crystal fibres, where similar ideas have been used to design confined electromagnetic waves [15], we expect one or several localized states to form at the location of the ‘defect’. The eigenfunctions ψ_n corresponding to localized states decay to zero within a finite distance from the defect, and it is again sufficient to solve Eq. (2) on a finite-size domain. The inset in Fig. 2 shows finite-element calculations of eigenfunctions corresponding to the two lowest eigenvalues for the geometrical ratio $d/\Lambda = 0.5$. The computed energy eigenvalues are converged with respect to an increase of the size of the domain on which Eq. (2) is solved. The two lowest eigenvalues correspond to localized states, whereas higher eigenvalues correspond to delocalized states (not shown). The second lowest eigenvalue is two-fold degenerate, and we only show one of the corresponding eigenstates. One ob-

*Electronic address: cf@mic.dtu.dk

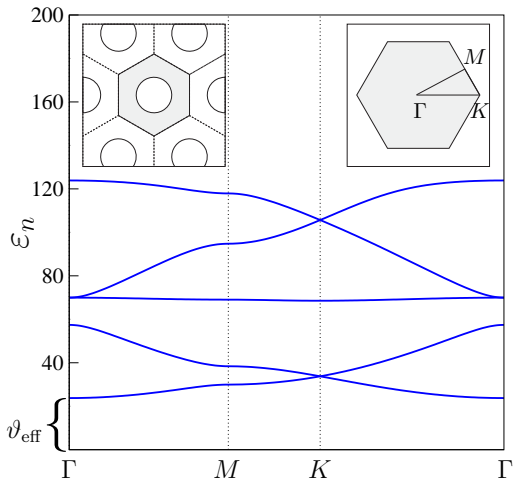


FIG. 1: (Color online) Bandstructure for the periodic structure. The ratio between the diameter of the anti-dots and the lattice constant is $d/\Lambda = 0.5$. Only the five lowest bands are shown. On the (dimensionless) energy axis we have indicated the gap ϑ_{eff} which can be considered as the height of an effective potential (see text). Left inset: Wigner-Seitz cell (grey area) for the periodic structure. Circles indicate anti-dots. Right inset: First Brillouin zone (grey area) with indications of the three high-symmetry axes along which the bandstructure was calculated.

serves that the shown eigenstate does not exhibit the underlying six-fold rotational symmetry of the lattice. This can be traced back to the fact that the mesh on which Eq. (2) was solved also lacked this symmetry. However, as recently shown by Mortensen *et al.* [16] even weak disorder in the lattice leads to a significant deformation of the higher-order eigenstates, and the shown eigenstate is thus likely to bear a closer resemblance to the states occurring in experimental structures, rather than the one found for an ideal lattice. Similarly, we note that the formation of defect states does not rely crucially on perfect periodicity of the anti-dot lattice, which thus allows for a certain tolerance in the fabrication of the anti-dot lattice.

Fig. 2 also shows finite-element calculations of the lowest eigenvalues corresponding to localized states as a function of the geometrical ratio d/Λ . In addition, the gap ϑ_{eff} as indicated on Fig. 1 is plotted as a function of d/Λ . The gap gives an upper limit to the existence of bound states and can be considered as the height of an effective two-dimensional spherical potential well in which the localized states reside. For GaAs with $d/\Lambda = 0.5$ and $\Lambda = 75$ nm the energy splitting of the two levels is $\Delta E = E_2 - E_1 \simeq 1.1$ meV which is much larger than $k_B T$ at sub-Kelvin temperatures. Thus, a missing single anti-dot in the lattice leads to the formation of a quantum dot with two levels at the location of the defect with an energy level structure suitable for a charge (orbital) qubit. As d/Λ is increased the confinement becomes stronger and the eigenvalues and their relative separations increase. Moreover, the number of

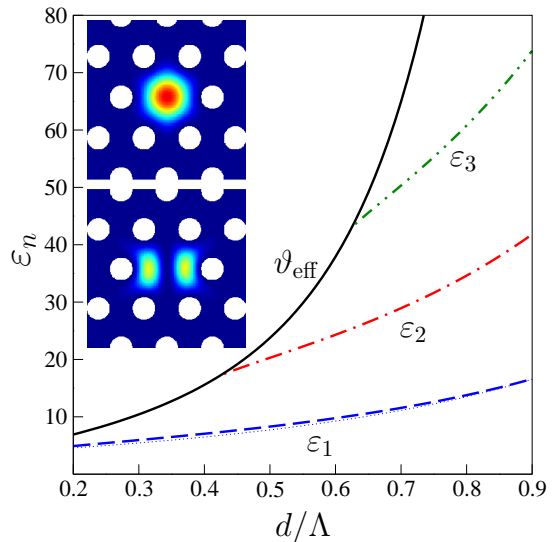


FIG. 2: (Color online) Energy spectrum for a single quantum dot. The three lowest dimensionless eigenvalues, ε_1 , ε_2 , ε_3 , (corresponding to localized states) as a function of the ratio between the anti-dot diameter d and the lattice constant Λ . The full line indicates the height ϑ_{eff} of the effective potential giving an upper limit to the existence of bound states (see text). The thin dotted line is the semi-analytic expression given in Eq. (3). Inset: Localized eigenfunctions $\psi_1(\mathbf{r})$ (upper panel) and $\psi_2(\mathbf{r})$ corresponding to the eigenvalues ε_1 and ε_2 , respectively, for $d/\Lambda = 0.5$. The absolute square $|\psi_i(\mathbf{r})|^2$, $i = 1, 2$, is shown.

levels in the quantum dot can be controlled by adjusting d/Λ , allowing for $n = 1, 2, 3, \dots$ levels in the quantum dot. In particular, for any $d/\Lambda < 0.42$ a single-level quantum dot is formed.

For sample optimizing purposes it is convenient to have simple expressions for the eigenvalues. In the limit of d/Λ approaching 1, the problem can be approximated with that of a two-dimensional spherical infinite potential well with radius $\Lambda - d/2$. For this problem the lowest eigenvalue is $\varepsilon_1^{(\infty)} = \Lambda^2 \alpha_{0,1}^2 / (\Lambda - d/2)^2$, where $\alpha_{0,1} \simeq 2.405$ is the first zero of the zeroth order Bessel function. Although this expression yields the correct scaling with d , the approximation obviously breaks down for small values of d/Λ . In that limit we follow the ideas of Glazman *et al.* [17] who studied quantum conductance through narrow constrictions. The effective one-dimensional energy barrier for transmission through two neighboring anti-dots has a maximum value of π^2 , and we thus approximate the problem with that of a two-dimensional spherical potential well of height π^2 and radius Λ . The lowest eigenvalue $\varepsilon_1^{(\pi^2)}$ for this problem can be determined numerically, and we find $\varepsilon_1^{(\pi^2)} \simeq 3.221$. Correcting for the

low- d/Λ behavior we find

$$\begin{aligned}\varepsilon_1 &\simeq \varepsilon_1^{(\infty)} - \lim_{d/\Lambda \rightarrow 0} \varepsilon_1^{(\infty)} + \varepsilon_1^{(\pi^2)} \\ &= \varepsilon_1^{(\pi^2)} + \frac{(4 - d/\Lambda)d/\Lambda}{(2 - d/\Lambda)^2} \alpha_{0,1}^2.\end{aligned}\quad (3)$$

In Fig. 2 we show this expression together with the results for the lowest eigenvalue determined by finite element calculations. As can be seen on the figure, the expression given above captures to a very high degree the results obtained from finite-element calculations. For the higher-order eigenvalues similar expressions can be found.

The leakage (transmission probability for penetrating the effective potential) due to a finite size of the anti-dot lattice can be found in the WKB approximation [18]. Multiplying by a characteristic attempt frequency we get the following estimate for the inverse life-time

$$\frac{1}{\tau_d(E)} \sim \sqrt{\frac{E}{2m^*\Lambda^2}} e^{-2N\Lambda\sqrt{\frac{2m^*}{\hbar^2}(V_{\text{eff}} - E)}} \quad (4)$$

where N is the number of rings of anti-dots surrounding the defect, and $V_{\text{eff}} = \vartheta_{\text{eff}}\hbar^2/2m^*\Lambda^2$. For GaAs with $\Lambda = 75$ nm, $d/\Lambda = 0.4$, and $N = 1, 2, 3, 4, 5$, respectively, we find $\tau_d \simeq 0.8$ ns, 0.3 μ s, 90 μ s, 30 ms, 10 s. We see that even relatively small ‘superlattices’ offer nearly perfect confinement.

We next consider the case where an anti-dot and one of its next-nearest neighbors have been left out of the lattice. Due to the close proximity of the resulting quantum dots, the different states of the two quantum dots couple with a coupling determined by the overlap of the corresponding single-dot wavefunctions. In particular, for two single-level quantum dots, L and R , with corresponding states $|L\rangle$ and $|R\rangle$, respectively, a bonding $|-\rangle = (|L\rangle - |R\rangle)/\sqrt{2}$ and an anti-bonding state $|+\rangle = (|L\rangle + |R\rangle)/\sqrt{2}$ form. The corresponding eigenenergies are $E_{\pm} = E \pm |t|$ with E being the eigenenergy corresponding to each of the states $|L\rangle$ and $|R\rangle$, and t being the tunnel matrix element. From the eigenenergy splitting we easily obtain the tunnel matrix element as $|t| = (E_+ - E_-)/2$.

The coupling of the two levels can be tuned using a metallic split gate defined on top of the 2DEG in order to control the opening connecting the two quantum dots. By increasing the applied gate voltage one squeezes the opening, thereby decreasing the overlap of the two states $|L\rangle$ and $|R\rangle$. In the following we model the split gate with an infinite potential barrier shaped as shown on the inset in Fig. 3. Changing the applied gate voltage effectively leads to a change of the width w of the opening, which we in the following take as a control parameter.

In Fig. 3 we show finite-element calculations of the dimensionless tunnel matrix element $|\tau| \equiv |t|\Lambda^2 2m^*/\hbar^2$ as a function of the geometrical ratio w/Λ for a number of different values of d/Λ in the single-level regime, *i.e.* $d/\Lambda < 0.42$. For GaAs with $\Lambda = 75$ nm and $d/\Lambda = 0.4$, $w/\Lambda = 0.6$, the tunnel matrix element is $|t| = 0.015$ meV.

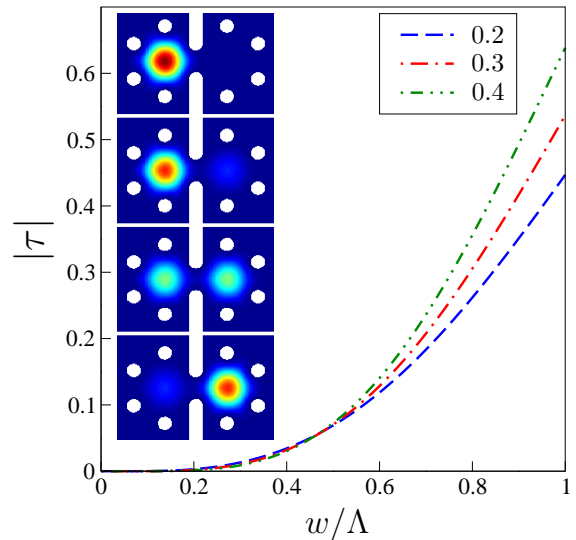


FIG. 3: (Color online) Coupling between two single-level quantum dots. The dimensionless tunnel matrix element $|\tau|$ as a function of the ratio between the width w of the opening defined by the split gates and the lattice constant Λ for different values of d/Λ (0.2, 0.3, 0.4) in the single-level regime. The width w is defined as the shortest distance between the split gates. Inset: Time propagation of an electron initially prepared in the state $|L\rangle$ (uppermost panel). Parameters are $d/\Lambda = 0.4$ and $w/\Lambda = 0.6$ which for GaAs with $\Lambda = 75$ nm implies an oscillation period of $T = 0.14$ ns (see text). The following panels show the state of the electron after a time span of $T/8, 2T/8, 3T/8$ (lowest panel), respectively. The absolute square $|\psi(\mathbf{r})|^2$ of the electron wavefunction is shown.

With this coupling an electron initially prepared in the state $|L\rangle$ is expected to oscillate coherently between $|L\rangle$ and $|R\rangle$ with a period of $T = h/2|t| = 0.14$ ns. We note that the period agrees well with the time scale set by the life-time obtained from Eq. (4) with $N = 1$. According to the figure the coupling varies over several orders of magnitude, thus clearly indicating that the coupling of the two quantum dots can be controlled via the applied gate voltage.

We have performed a numerical time propagation of an electron initially prepared in the state $|L\rangle$. In the inset of Fig. 3 we show a number of snapshots at different points in time as the electron propagates from the left to the right quantum dot. Once located in the right quantum dot, the electron starts propagating back to the left quantum dot (not shown), confirming the expected oscillatory behavior.

Considering the double-dot as a charge qubit, one-qubit operations may be performed by controlling the tunnel matrix element as described above. Alternatively, one may consider the spin of two electrons, each localized on one of the quantum dots, as qubits. In that case the qubits (the spins) couple due to the exchange coupling, which again depends on the amplitude for tunneling between the two quantum dots. In this manner one may

perform two-qubit operations as originally proposed in Ref. [1].

In this work we have carried out a number of model calculations showing that an implementation of qubits using defect states in an anti-dot lattice is feasible. While we have here only considered the most basic building blocks of a quantum computer, a single charge qubit or two spin-qubits, we believe that the suggested structure can readily be scaled to a larger number of qubits. It is not difficult to imagine large architectures consisting of an anti-dot lattice with several coupled defect states and/or linear arrays of defect states constituting quantum channels along which coherent and controllable transport of electrons can take place [19]. We believe that the sug-

gested structure, when compared to conventional gate-defined quantum dots, has the advantage that less wiring is needed. The individual antidots need not be electrically contacted, which in the case of conventional gate-defined structures may be a critical issue for large structures consisting of many quantum dots.

In conclusion, we have suggested a new structure which seems to offer many attractive features in terms of flexibility, scalability, and operation in the pursuit of achieving solid state quantum computation.

The authors would like to thank D. Graf, P. E. Lindelof, and T. Novotný for valuable advice during the preparation of the manuscript, and T. Markussen for sharing his numerical codes with them.

-
- [1] D. Loss and D. P. DiVincenzo, *Phys. Rev. A* **57**, 120 (1998).
- [2] T. Fujisawa, T. H. Oosterkamp, W. G. van der Wiel, B. W. Broer, R. Aguado, S. Tarucha, and L. P. Kouwenhoven, *Science* **282**, 932 (1998).
- [3] J. M. Elzerman, R. Hanson, J. S. Greidanus, L. H. W. van Beveren, S. de Franceschi, L. M. K. Vandersypen, S. Tarucha, and L. P. Kouwenhoven, *Phys. Rev. B* **67** (2003).
- [4] T. Hayashi, T. Fujisawa, H. D. Cheong, Y. H. Jeong, and Y. Hirayama, *Phys. Rev. Lett.* **91** (2003).
- [5] J. Gorman, D. G. Hasko, and D. A. Williams, *Phys. Rev. Lett.* **95**, 090502 (2005).
- [6] A. C. Johnson, J. R. Petta, J. M. Taylor, A. Yacoby, M. D. Lukin, C. M. Marcus, M. P. Hanson, and A. C. Gossard, *Nature* **435**, 925 (2005).
- [7] D. P. DiVincenzo, *Fortschr. Phys.* **48**, 771 (2000).
- [8] P. R. Gerhardt, D. Weiss, and K. von Klitzing, *Phys. Rev. Lett.* **62**, 1173 (1989).
- [9] D. R. Hofstadter, *Phys. Rev. B* **14**, 2239 (1976).
- [10] T. O. Stadelmann and R. J. Nicholas, in *Microscopy of Semiconducting Materials 2003* (2003), no. 180 in *Inst. Phys. Conf. Ser.*, pp. 661 – 664.
- [11] M. Cavallini, P. Mei, F. Biscarini, and R. Garcia, *Appl. Phys. Lett.* **83**, 5286 (2003).
- [12] The choice of material is not crucial for the conclusions reached below, and other choices of material, *e.g.* materials with a lower effective mass, may be preferable.
- [13] This assumption corresponds to taking the limit $V_0 \rightarrow \infty$. We believe that our results do not change qualitatively for a large but finite value of V_0 . The appealing and convenient form of Eq. (2) can however only be obtained in the limit $V_0 \rightarrow \infty$.
- [14] Femlab, <http://www.comsol.com>.
- [15] N. A. Mortensen, *Opt. Lett.* **30**, 1455 (2005).
- [16] N. A. Mortensen, M. D. Nielsen, J. R. Folkenberg, K. P. Hansen, and J. Lægsgaard, *J. Opt. A: Pure Appl. Opt.* **6**, 221 (2004).
- [17] L. I. Glazman, G. K. Lesovik, D. E. Khmel'nitskii, and R. I. Shekter, *JETP Lett.* **48**, 238 (1988).
- [18] M. Koshiha and K. Saitoh, *Opt. Commun.* **253**, 95 (2005).
- [19] G. M. Nikolopoulos, D. Petrosyan, and P. Lambropoulos, *Europhys. Lett.* **65**, 297 (2004).